49th IEEE Conference on Decision and Control
December 15-17, 2010
Hilton Atlanta Hotel, Atlanta, GA, USA

Semiparametric Identification of Hammerstein Systems Using Input Reconstruction and a Single Harmonic Input

Anthony M. D'Amato, Kenny S. Mitchell, Bruno O. S. Teixeira, and Dennis S. Bernstein

Abstract— **We present a two-step method for identifying SISO Hammerstein systems. First, using a persistent input with retrospective cost optimization, we estimate a parametric model of the linear system. Next, we pass a single harmonic signal through the system. We use l-delay input reconstruction with the parametric model of the linear system to estimate the inaccessible intermediate signal. Using the estimate of the intermediate signal we estimate a nonparametric model of the static nonlinearity, which is assumed to be only piecewise continuous. This method is demonstrated on several numerical and experimental examples of increasing complexity.**

I. Introduction

Nonlinear model structures involving a single linear dynamic block and a single nonlinear static block comprise a natural first step in nonlinear system identification. A nonlinear mapping at the input yields a Hammerstein model, while a nonlinear mapping at the output yields a Wiener model. The literature on system identification for these models structures is extensive, and shows that nonlinear system identification for these problems remains a challenging and useful area of research. Representative references on Hammerstein and Wiener system identification include [1, 4, 10] and [1–5], respectively.

The starting point for the present paper on Hammerstein-system identification is the semiparametric approach developed in [5] for identifying Wiener systems. This approach involves two steps and is semiparametric, which, as described in [6], refers to the fact that the nonlinear block is estimated nonparametrically, whereas the linear dynamics are identified parametrically. In the first step, a single harmonic is applied to the system to determine the phase shift of the output of the linear system relative the input to the linear system; this information is then used to construct a nonparametric approximation of the nonlinearity. Next, using knowledge of the output nonlinearity, which is not assumed to be invertible, retrospective cost optimization (RCO) is used to estimate the parameters of the linear model. RCO was originally developed for adaptive control [7, 8, 11], and has subsequently been applied to various identification problems, including model refinement [5, 9].

In the present paper we develop a two-step semiparametric technique for identifying single-input, single-output (SISO) Hammerstein systems. In the first step we use a sufficiently rich signal to estimate the linear dynamics of the system. We then use retrospective cost optimization to estimate the parametric model of the linear dynamics, although alternative techniques [14] can be used for this step, such as output-error modeling methods. When an initial model of the linear system is available, retrospective cost optimization can utilize this information. In the present paper we do not assume that an initial model is available.

For the second step, we apply a single harmonic input signal, and measure the output once the trajectory of the system reaches steady state. We then use input reconstruction, which is based on l-delay left invertibility of the linear parametric model [12]. By using input reconstruction with the identified linear parametric model, we estimate the inaccessible intermediate signal. We examine the estimate of the intermediate signal (which is not harmonic due to the nonlinearity) relative to the input, and use the symmetry properties of these signals to estimate the nonharmonic phase shift. This estimate allows us to infer the phase shift of the unmeasured intermediate signal (that is, the output of the nonlinearity) and thus reconstruct this signal up to an arbitrary amplitude. By plotting the reconstructed intermediate signal versus the input signal, we thus obtain a nonparametric approximation of the nonlinear block of the system.

The contents of the paper are as follows. In Section 2 we define the Hammerstein identification problem. A method for parametric identification of the linear time-invariant dynamics using retrospective cost optimization is reviewed in Section 3, while a method for nonparametric identification of the static nonlinearity using input reconstruction and single harmonic input is presented in Section 4. These methods are demonstrated on numerical and experimental examples in sections 5 and 6, respectively. Concluding remarks are presented in Section 7.

II. Problem Formulation

Consider the block-structured Hammerstein model shown in Figure 1a, with input $u(k) \in \mathbb{R}$ and intermediate signal

$$v(k) = \mathcal{H}(u(k)), \tag{1}$$

where $\mathcal{H} : \mathbb{R} \longmapsto \mathbb{R}$ is the static nonlinearity, and $\mathcal{L}$ is the SISO discrete-time linear time-invariant dynamic system

$$x(k+1) = Ax(k) + Bv(k), \tag{2}$$

$$y(k) = Cx(k), \tag{3}$$

This work was supported in part by NASA through grants NNX08AB92A and NNX08BA57A, USA, and by FAPEMIG, Brazil.

A. M. D'Amato, K. S. Mitchell and D. S. Bernstein are with the Department of Aerospace Engineering, University of Michigan, Ann Arbor, MI, USA. {amdamato, ksmitch, dsbaero}@umich.edu

B. O. S. Teixeira is with the Department of Electronic Engineering, Federal University of Minas Gerais, Belo Horizonte, MG, Brazil. brunoot@ufmg.br

where $y(k) \in \mathbb{R}$ is the output, $x(k) \in \mathbb{R}^n$ is the state vector, and k is the sample index.

We assume that $\mathcal{L}$ is asymptotically stable and $\mathcal{H}$ is piecewise continuous. Note that we do not assume that $\mathcal{H}$ is invertible, one-to-one, continuous, or $\mathcal{H}(0) = 0$. Also, we assume that $v(k)$ is not accessible, and that $x(0)$ is unknown and possibly nonzero.

Figure 1b shows the scaled-domain modification $\mathcal{L}_\lambda(\nu) \triangleq \mathcal{L}\left(\frac{\nu}{\lambda}\right)$ of $\mathcal{L}$, where λ is a nonzero real number. Therefore, $\mathcal{L}_\lambda(\lambda v) = \mathcal{L}(v)$. Each value of λ scales both the gain of $\mathcal{L}$ and the domain of $\mathcal{H}$. However, λ is not identifiable.

(a) (b)

Fig. 1. (a) Block-structured Hammerstein model, where u is the input, v is the intermediate signal, y is the output, $\mathcal{H}$ is a static nonlinearity, and $\mathcal{L}$ is a discrete-time linear time-invariant dynamic system. (b) An equivalent scaled model, where λ is a scaling factor and $\mathcal{L}_\lambda$ is a scaled-domain modification of $\mathcal{L}$ satisfying $\mathcal{L}_\lambda(\lambda v) = \mathcal{L}(v)$. The scaling factor λ is not identifiable.

III. Parametric Identification of the Linear Time-Invariant Dynamics

Using a sufficiently rich input u and measuring the output y of the Hammerstein system, we identify a model of $\mathcal{L}$ given by $\hat{\mathcal{L}}$ using retrospective cost optimization (RCO). The RCO algorithm is presented in [9] together with guidelines for choosing its tuning parameters, namely, n_c, p, and α. We do not assume that the initial state of $\mathcal{L}$ is zero.

Consider the adaptive feedback architecture for $\hat{\mathcal{L}}$ shown in Figure 2, where $\hat{\mathcal{L}}_{\mathrm{m}}$ denotes the initial model with input $w \in \mathbb{R}$ and output $\hat{y} \in \mathbb{R}$, and where $\hat{\mathcal{L}}_\Delta$ denotes the feedback delta model with inputs u, $\hat{y} \in \mathbb{R}$ and output w. The goal is to adaptively tune $\hat{\mathcal{L}}_\Delta$ so that the performance variable

$$z(k) \triangleq y(k) - \hat{y}(k) \tag{4}$$

is minimized in the presence of the identification signal u. For simplicity, we choose $\hat{\mathcal{L}}_{\mathrm{m}}$ to be the one-step delay $1/\mathbf{z}$. In the case that information is known about the linear system, an initial model can be used in place of the unit delay.

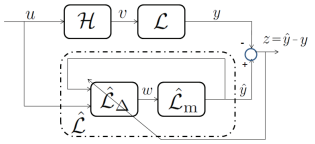

Fig. 2. Identification architecture for Hammerstein models using RCO.

When an initial model of the linear system is not available, various system identification methods can be used to obtain the parametric estimate of $\mathcal{L}$, such as output-error modeling methods [14]; see Example 6.3. To identify a parametric model $\hat{\mathcal{L}}$ for the linear system using the signals u and y, we assume that $\mathcal{H}$ is approximately linear for the domain of u used to drive y. In a sense, we ignore the nonlinearity $\mathcal{H}$, the validity of this assumption is investigated in [15].

IV. Nonparametric Identification of the Static Nonlinearity

Consider the harmonic input signal

$$u(k) = A_0 \sin(\omega_0 k T_s) = A_0 \sin(\Omega_0 k), \tag{5}$$

where A_0 is the amplitude, ω_0 is the angular frequency in rad/sec, T_{s} is the sample period in sec/sample, and $\Omega_0 \triangleq \omega_0 T_{\mathrm{s}}$ is the angular sample frequency in rad/sample. The intermediate signal is

$$v(k) = \mathcal{H}(u), \tag{6}$$

and the output signal is

$$y(k) = G(\mathbf{z})\mathcal{H}(u), \tag{7}$$

where $G(\mathbf{z}) = C(\mathbf{z}I - A)^{-1}B$ is a transfer function representation of $\mathcal{L}$. To obtain the nonparametric estimate $\hat{\mathcal{H}}$ of the nonlinearity $\mathcal{H}$, we require an estimate $\hat{v}(k)$ of the inaccessible intermediate signal $v(k)$. To obtain $\hat{v}(k)$, we use input reconstruction [12, 13]. Together, $\hat{\mathcal{L}}$ and $\hat{\mathcal{H}}$ comprise a *semiparametric model* of the Hammerstein system.

A. Input Reconstruction

With an estimate $\hat{\mathcal{L}}$ of the linear system $\mathcal{L}$, we pass (5) through (1)-(3). Next we wish to obtain an estimate $\hat{v}$ of the intermediate signal v. To obtain $\hat{v}$, we use input reconstruction, which depends on the l-delay invertibility of the estimate of $G(\mathbf{z})$.

Let l be a nonnegative integer. Then $G(\mathbf{z})$ is *l-delay invertible* if there exists a proper transfer function $G_l(\mathbf{z})$ (called an *l-delay inverse of* $G(\mathbf{z})$) such that $G_l(\mathbf{z})G(\mathbf{z}) = \mathbf{z}^{-l}$ for almost all $\mathbf{z} \in \mathbb{C}$ [12]. For a SISO system, G is l-delay invertible for all $l \geq d$, where d is the relative degree of $G(\mathbf{z})$.

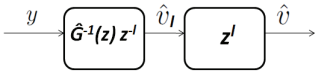

Fig. 3. Input reconstruction. Using l-delay invertibility of the estimated linear system, the intermediate signal can be reconstructed.

Using input reconstruction we obtain

$$\hat{v}_l(k) = \hat{G}^{-1}(\mathbf{z})\mathbf{z}^{-l}y(k), \tag{8}$$

where $\hat{v}_l(k) = \hat{v}(k-l)$ for $k \geq l$. For the case $l = d$, the estimate $\hat{v}(k)$ is in nonharmonic phase with the true intermediate signal $v(k)$, where nonharmonic phase is defined in Section IV-D. We also consider the case $l \neq d$, since d is not assumed to be known. Using the harmonic input u and $\hat{v}$ we can determine the nonharmonic phase shift, and then determine an estimate of the nonparametric map of the nonlinearity.

B. Signal Symmetry

Note that the continuous-time harmonic signal $\sin(\omega_0 t)$ is symmetric in the intervals $\left[0, \frac{1}{2}T_0\right]$ and $\left[\frac{1}{2}T_0, T_0\right]$ about the points $\frac{1}{4}T_0$ and $\frac{3}{4}T_0$, respectively, where $T_0 \triangleq \frac{2\pi}{\omega_0}$ is the period of the harmonic input. To preserve symmetry for the sampled signal (5) about the points $\frac{1}{4}T_0$ and $\frac{3}{4}T_0$, we assume that $\Omega_0 = \frac{\pi}{2m}$, where m is a positive integer. Thus $N_0 \triangleq 4m = \frac{T_0}{T_s}$ is the period of the discrete-time input (5). With this choice of Ω_0, the sampled signal $u(k)$ is symmetric in the intervals $\left[0, \frac{1}{2}N_0\right]$ and $\left[\frac{1}{2}N_0, N_0\right]$ about the points $\frac{1}{4}N_0$ and $\frac{3}{4}N_0$, respectively. Furthermore, $q \triangleq d - l$ is an integer, that is, the estimated intermediate signal $\hat{v}(k)$, which is shifted relative to $u(k)$ due to $d-l$, the error in the relative degree between $\mathcal{L}$ and $\hat{\mathcal{L}}$, is symmetric about $\frac{1}{4}N_0 + q$ in the interval $\left[q, \frac{1}{2}N_0 + q\right]$ and about $\frac{3}{4}N_0 + q$ in the interval $\left[\frac{1}{2}N_0 + q, N_0 + q\right]$.

Next, we note that the intermediate signal v, which is not generally harmonic, possesses the same symmetry as u on the same intervals. By exploiting knowledge of this symmetry, we can identify the *nonharmonic phase shift* of $\hat{v}$ relative to u. Since $\hat{v}$ is not sinusoidal, the nonharmonic phase shift of $\hat{v}$ relative to u refers to the shifting of the symmetric portions of $\hat{v}$ relative to the symmetric portions of u. Knowledge of this nonharmonic phase shift allows us to determine v up to a constant multiple, specifically, $\hat{v}$ is shifted relative to u by a known number of samples.

To clarify the above discussion, we present two examples using $A_0 = 1$, $m = 18$ (so that $\Omega_0 = \pi/36$). First, consider the polynomial nonlinearity $v = \mathcal{H}(u) = 0.6(u+1)^3 - 1$, which is neither even nor odd. Figure 4a illustrates the resulting signals $u(k)$, $v(k)$, $\hat{v}(k)$ in harmonic steady state, where the delay q, between $v(k)$ and $\hat{v}(k)$, is added to simulate modeling inaccuracy. Note that u and v are symmetric about the discrete-time index δ in the interval $\left[\delta - \frac{1}{4}N_0, \delta + \frac{1}{4}N_0\right]$ and about $\delta + \frac{1}{2}N_0$ in the interval $\left[\delta + \frac{1}{4}N_0, \delta_2 + \frac{3}{4}N_0\right]$. Likewise, $\hat{v}$ is symmetric about the discrete-time index ε in the interval $\left[\varepsilon - \frac{1}{4}N_0, \varepsilon + \frac{1}{4}N_0\right]$ and about $\varepsilon + \frac{1}{2}N_0$ in the interval $\left[\varepsilon + \frac{1}{4}N_0, \varepsilon + \frac{3}{4}N_0\right]$.

Second, we consider the even polynomial nonlinearity $v = \mathcal{H}(u) = u^2$. Figure 4b illustrates the resulting signals $u(k)$, $v(k)$, and $\hat{v}(k)$ in harmonic steady state. The signal u of Figure 4b is equal to the signal u shown in Figure 4a. However, in addition to the two points of symmetry shown in Figure 4a, note that v and $\hat{v}$ have two additional points of symmetry, specifically, v is symmetric about $\delta + \frac{1}{4}N_0$ in the interval $\left[\delta, \delta + \frac{1}{2}N_0\right]$ and about $\delta + \frac{3}{4}N_0$ in the interval $\left[\delta + \frac{1}{2}N_0, \delta + N_0\right]$, and $\hat{v}$ is symmetric about $\varepsilon + \frac{1}{4}N_0$ in the interval $\left[\varepsilon, \varepsilon + \frac{1}{2}N_0\right]$ and about $\varepsilon + \frac{3}{4}N_0$ in the interval $\left[\varepsilon + \frac{1}{2}N_0, \varepsilon + N_0\right]$.

C. Symmetry Search Algorithm

We now review from [5] an algorithm for determining ε from $\hat{v}$. We then use ε to estimate the nonharmonic phase shift of $\hat{v}$ relative to u. For convenience, we assume that

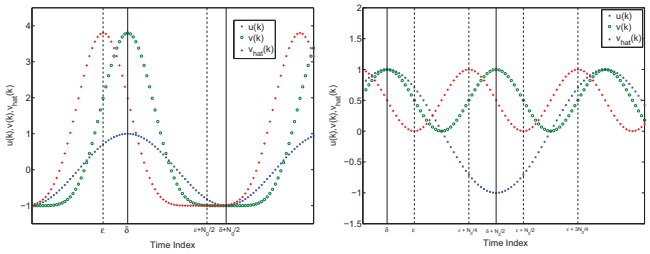

(a) (b)

Fig. 4. Illustration of the symmetry properties of the signals u, v, and $\hat{v}$. For (a) the non-even polynomial nonlinearity is $v = \mathcal{H}(u) = 0.6(u+1)^3 - 1$ and (b) the even polynomial nonlinearity is $v = \mathcal{H}(u) = u^2$. For both cases, u and v are symmetric about δ in the interval $\left[\delta - \frac{1}{4}N_0, \delta + \frac{1}{4}N_0\right]$ and about $\delta + \frac{1}{2}N_0$ in the interval $\left[\delta + \frac{1}{4}N_0, \delta + \frac{3}{4}N_0\right]$, while $\hat{v}$ is symmetric about ε in the interval $\left[\varepsilon - \frac{1}{4}N_0, \varepsilon + \frac{1}{4}N_0\right]$ and about $\varepsilon + \frac{1}{2}N_0$ in the interval $\left[\varepsilon + \frac{1}{4}N_0, \varepsilon + \frac{3}{4}N_0\right]$. In addition, for the case of an even polynomial nonlinearity shown in (b), v and $\hat{v}$ have two additional points of symmetry, specifically, v is symmetric about $\delta + \frac{1}{4}N_0$ in the interval $\left[\delta, \delta + \frac{1}{2}N_0\right]$ and about $\delta + \frac{3}{4}N_0$ in the interval $\left[\delta + \frac{1}{2}N_0, \delta + N_0\right]$, and $\hat{v}$ is symmetric about $\varepsilon + \frac{1}{4}N_0$ in the interval $\left[\varepsilon, \varepsilon + \frac{1}{2}N_0\right]$ and about $\varepsilon + \frac{3}{4}N_0$ in the interval $\left[\varepsilon + \frac{1}{2}N_0, \varepsilon + N_0\right]$.

the harmonic steady state begins at $k = 0$. Consider the signal $\hat{v}$ shown in Figure 5, and let $n \geq 6m$ denote the width of the data window so that it includes at least one and a half periods. To encompass a complete signal period, we construct a sliding window with $N_0 + 1$ data points. The window is divided into quarters as shown in Figure 5.

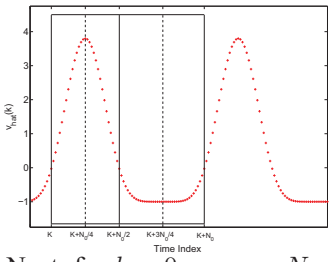

5. Illustration of the symmetry search algorithm. The solid line box comprises the sliding window of length $N_0 + 1$ starting at time k, while the dashed lines indicate the windowed points of symmetry.

Next, for $k = 0, \ldots, n - N_0$, define

$$\beta_1(k) \triangleq \sum_{i=1}^{2m-1} \left|\hat{v}\left(k + i - 1\right) - \hat{v}\left(k + 2m - i + 1\right)\right|, \quad (9)$$

which is the sum of the absolute difference in magnitude for each pair of candidate symmetric points in the first and second quarters about the point $k + \frac{1}{4}N_0$ for the sliding window starting at time step k. Likewise, for $k = 0, \ldots, n - N_0$, define

$$\beta_2(k) \triangleq \sum_{i=1}^{2m-1} \left|\hat{v}\left(k + 2m + i - 1\right) - \hat{v}\left(k + 4m - i + 1\right)\right|, \quad (10)$$

for each pair of candidate symmetric points in the third and fourth quarters about the point $k + \frac{3}{4}N_0$. The values of β_1 and β_2 quantify the symmetry error about the points $k + \frac{1}{4}N_0$ and $k + \frac{3}{4}N_0$, respectively, for each allowable value of k. Thus, using (9) and (10), we define the *symmetry error index* $\beta(k) \triangleq \beta_1(k) + \beta_2(k)$, corresponding to the sliding window

starting at point k, for $k = 0, \ldots, n - N_0$.

For $k = 0, \ldots, n - N_0$, let $k_0 < N_0$ be the minimizer of $\beta(k)$. We use knowledge of k_0 to determine the location of the points of symmetry ε and $\varepsilon + \frac{1}{2}N_0$ for the sliding window starting at point k_0. In particular, since k_0 is the starting point of the window that minimizes β and since ε and $\varepsilon + \frac{1}{2}N_0$ are, respectively, the quarter point and three quarter point of the same window, it follows that

$$\varepsilon = k_0 + \frac{1}{4}N_0, \quad \varepsilon + \frac{1}{2}N_0 = k_0 + \frac{3}{4}N_0. \tag{11}$$

To illustrate the symmetry search algorithm, we reconsider the example considered in Figures 4a and 5, where $v = \mathcal{H}(u) = 0.6(u+1)^3 - 1$. Note that $\mathcal{H}$ is not even. Figure 6a shows the values of β calculated for $\hat{v}(k)$ on the interval $[k_0, k_0 + 2N_0]$. Since, in Figure 6a, the data window of $\hat{v}(k)$ is selected to start at $k_0 = \varepsilon - \frac{1}{4}N_0$, the minimum values of $\beta(k)$ occur at k_0 and $k_0 + N_0$, where $k_0 + N_0$ is the start of the next period and, thus, need not be considered. Thus, using the unique minimizer k_0 of $\beta(k)$, it follows that the locations of the points of symmetry are given by (11).

Next, for the even nonlinearity $v = \mathcal{H}(u) = u^2$ considered in Figure 4b, Figure 6b shows the values of $\beta(k)$ calculated for $v(k)$ on the interval $[k_0, k_0 + 2N_0]$. In this case, the minimum values of $\beta(k)$ occur at k_0, $k_0 + \frac{1}{2}N_0$, and $k_0 + N_0$, where $k_0 + N_0$ is the start of the next period and, thus, need not be considered. Thus, using k_0, it follows that the locations of the points of symmetry are given by (11). Also, using $k_0 + \frac{1}{2}N_0$, we obtain two additional points of symmetry given by

$$\varepsilon + \frac{1}{4}N_0 = k_0 + \frac{1}{2}N_0, \quad \varepsilon + \frac{3}{4}N_0 = k_0 + N_0. \tag{12}$$

This ambiguity is due to the fact that ε and $\varepsilon + \frac{1}{2}N_0$ are the midpoints of two identical symmetric portions of $\hat{v}$. Thus, the start of the data window within which the function has the symmetry properties illustrated in Figure 5 can be taken as either k_0 or $k_0 + \frac{1}{2}N_0$. Note that the second minimizer $k_0 + \frac{1}{2}N_0$ appears only for even nonlinearities.

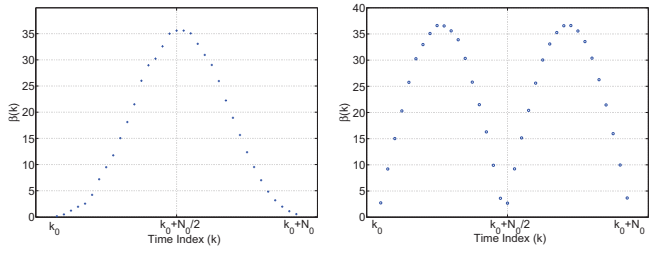

Fig. 6. Illustration of the symmetry error index $\beta(k)$ given by (9). The values of $\beta(k)$ are shown for two static nonlinearities, namely, (a) a non-even polynomial and (b) an even polynomial.

D. Nonparametric Approximation of the Static Nonlinearity

Using δ, which is assumed to be known from the harmonic input u, and the estimate of ε obtained from $\hat{v}$ in Section IV-C, we now determine an estimate $\hat{\phi}$ of the nonharmonic phase shift of $\hat{v}$ relative to u by $\hat{\phi} \triangleq \Omega_0(\varepsilon - \delta)$, which is an estimate of $d - l$. Moreover, define the virtual signal

$$\tilde{v}(k) \triangleq \hat{v}\left(k + \frac{\hat{\phi}}{\Omega_0}\right), \tag{13}$$

which is an approximation of the intermediate signal v. Note that the amplitude of $\tilde{v}(k)$ is irrelevant due to the scaling factor λ shown in Figure 1b. Using $\tilde{v}$ and u, the nonparametric estimate of $\mathcal{H}$ is given by

$$\hat{\mathcal{H}} \triangleq \{(u(k_0), \tilde{v}(k_0)), (u(k_0+1), \tilde{v}(k_0+1)), \ldots, (u(n), \tilde{v}(n))\}, \tag{14}$$

where each pair $(u(k), \tilde{v}(k),)$, for $k = 0, \ldots, n$, determines a value of the nonparametric estimate $\hat{\mathcal{H}}$ of $\mathcal{H}$.

Figure 6 shows that, depending on the type of nonlinearity, $\beta(k)$ has either one or two minima within each period. For a non-even polynomial nonlinearity, $\beta(k)$ has one minimum within each period. Therefore, the estimate of the nonharmonic phase shift has two candidate values, namely, $\hat{\phi}$ and $\hat{\phi} + \pi$. For an even nonlinearity, $\beta(k)$ has two minima within each period. Therefore, the estimate of the nonharmonic phase shift has four candidate values, namely, $\hat{\phi}$, $\hat{\phi} + \frac{\pi}{2}$, $\hat{\phi} + \pi$, and $\hat{\phi} + \frac{3\pi}{2}$. However, for the even case, $\hat{\phi}$ and $\hat{\phi} + \pi$ yield the same nonparametric model $\hat{\mathcal{H}}$, while $\hat{\phi} + \frac{\pi}{2}$ and $\hat{\phi} + \frac{3\pi}{2}$ yield the same $\hat{\mathcal{H}}$.

Therefore, in both the non-even and even cases, there are two candidate nonparametric estimates of $\mathcal{H}$, both of which are constructed using (13) and (14). In practice q is small compared to N_0, therefore, it is reasonable to assume that ϕ is the correct nonharmonic phase shift candidate for estimating $\mathcal{H}$.

V. Simulated Examples

To demonstrate semiparametric Hammerstein model identification, we consider two static nonlinearities, namely, a non-even case and an even case. For both examples, we choose G to have poles $0.34 \pm 0.87\jmath, -0.3141 \pm 0.9\jmath, 0.05 \pm 0.3122\jmath, -0.6875$ and zeros $0.14 \pm 0.97\jmath, -0.12 \pm 0.62\jmath, -0.89$ with monic numerator and denominator. Also, $u(k)$ is chosen to be a realization of zero-mean Gaussian white noise with standard deviation $\sigma_u = 3.5$.

Example 5.1: (Non-even Polynomial) Consider $\mathcal{H}$ defined by

$$v = \mathcal{H}(u) = u^3 + 4u + 7. \tag{15}$$

The parameters for nonparametric identification of $\mathcal{H}$ are $m = 500$ and $A_0 = 5$. Figure 7a shows the frequency response of the true dynamic model G and the identified model using RCO. The RCO parameters used to identify the linear dynamic system are set as $n_c = 9$, $p = 1$, and $\alpha = 1$. Figure 7b compares the true nonlinearity with the identified nonlinearity estimated using input reconstruction.

Example 5.2: (Even Polynomial) Consider $\mathcal{H}$ defined by

$$v = \mathcal{H}(u) = 7u^4 + u^2. \tag{16}$$

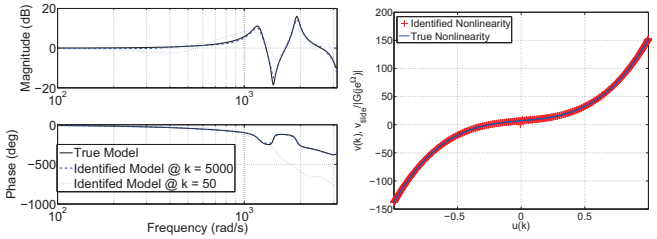

(a) (b)

Fig. 7. (a) Frequency response comparison of the true G and the identified LTI system, where k is the number of data points used to determine the identified model. For $k = 5000$, the traces for the true and identified models almost coincide. (b) Identified nonlinearity versus true nonlinearity, where $m = 500$ and $A_0 = 5$. The argument of the identified nonlinearity is scaled by $\frac{1}{|G(e^{j\Omega_0})|}$ to facilitate comparison with the true nonlinearity (15)

The parameters for nonparametric identification of $\mathcal{H}$ are $m = 500$ and $A_0 = 5$. Figure 8a shows the frequency response of the true dynamic model G and the identified model using RCO. The RCO parameters used to identify the linear dynamic system are set as $n_c = 9$, $p = 1$, and $\alpha = 1$. Figure 8b compares the true nonlinearity (blue line) with the identified nonlinearity estimated using input reconstruction (red crosses).

To illustrate the ambiguity discussed in Section IV-D, we select the incorrect nonharmonic phase shift, specifically, $\hat{\phi} + \frac{\pi}{2}$, which is represented by the black circles in Figure 8b. Note that the incorrect nonharmonic phase shift produces an erroneous nonparametric model of the nonlinearity.

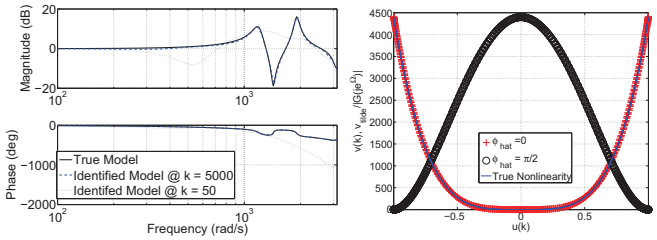

(a) (b)

Fig. 8. (a) Frequency response comparison of the true G and the identified LTI system, where k is the number of data points used to determine the identified model. (b) Identified nonlinearities versus true nonlinearity, where $m = 500$ and $A_0 = 5$. The argument of the identified nonlinearity is scaled by $\frac{1}{|G(e^{j\Omega_0})|}$ to facilitate comparison with the true nonlinearity (16). The red crosses represent the identified nonlinearity, the black circles, represent the identified nonlinearity using the incorrect nonharmonic phase shift.

VI. Experimental Examples

We now present experimental examples using a resistor-inductor-capacitor (RLC) circuit. The true parametric model of the RLC circuit is generated from first principles, where $R = 250\ \Omega$. $L = 55$ mH, $C = 23.5\ \mu$F, and

$$\dot{x} = \begin{bmatrix} 0 & 1 \\ \frac{-1}{LC} & \frac{-R}{L} \end{bmatrix} x + \begin{bmatrix} 0 \\ \frac{1}{L} \end{bmatrix} v, \tag{17}$$

$$y = \begin{bmatrix} 0 & R \end{bmatrix} x, \tag{18}$$

where $x \in \mathbb{R}^2$ is the state vector, which is the circuit charge and current. For the following examples, G is a discrete time transfer function representation of (17)–(18), with a sampling rate of $Ts = 0.0001$. Figure 9a shows the RLC circuit, where the nonlinearity is a saturation in the actuation voltage.

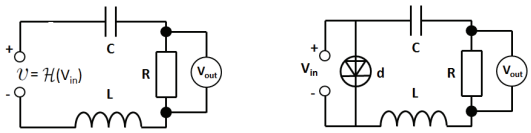

(a) (b)

Fig. 9. (a) Block diagram representation of the series RLC circuit, where the input voltage is modified by $\mathcal{H}$. For this example, $\mathcal{H}$ is a saturation function. (b)A series RLC circuit in parallel with a diode. The resulting system is a Hammerstein system where the diode can be represented as a static nonlinearity and the series RLC circuit is the linear model.

Example 6.1: (Saturation) Consider $\mathcal{H}$ defined by

$$v = \mathcal{H}(u) = \begin{cases} u, & \text{if } -1 < u < 1; \\ 1, & \text{if } u \geq 1; \\ -1, & \text{if } u \leq 1. \end{cases} \tag{19}$$

The parameters for nonparametric identification of $\mathcal{H}$ are $m = 500$ and $A_0 = 5$. Figure 10a shows the frequency response of the true dynamic model G, and the identified model using RCO. The RCO parameters used to identify the linear dynamic system are set as $n_c = 9$, $p = 1$, and $\alpha = 1$. Figure 10b compares the true nonlinearity with the identified nonlinearity estimated using input reconstruction.

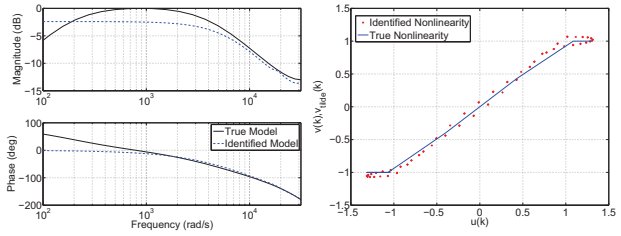

(a) (b)

Fig. 10. (a) Frequency response comparison of the true G and the identified LTI system, where k is the number of data points used to determine the identified model. For $k = 5000$, the traces for the true and identified models almost coincide. (b) Identified nonlinearity versus true nonlinearity, where $m = 500$ and $A_0 = 5$. The argument of the identified nonlinearity is scaled by $\frac{1}{|G(e^{j\Omega_0})|}$ to facilitate comparison with the true nonlinearity (19).

We now reconsider the RLC circuit in Figure 9b, where a diode is presented in parallel with the circuit. The diode modifies the input voltage according to a nonlinear function $\mathcal{H}$. We first determine $\mathcal{H}$ experimentally, using a circuit where the diode is the sole component. $\mathcal{H}$ is approximatively given by

$$v = \mathcal{H}(u) = \begin{cases} u, & \text{if } u < 0.07; \\ 0.07, & \text{if } u \geq 0.07. \end{cases} \tag{20}$$

We view (20) as the truth model of $\mathcal{H}$.

Example 6.2: (Diode in Parallel with RLC Circuit) Consider $\mathcal{H}$ which is given by (20), which is in parallel with the linear dynamic system given by (17) and (18). In this example, the diode is assumed to be inaccesible, namely, it can not be directly measured. The RCO parameters used to identify the linear dynamic system are set as $n_c = 3$, $p = 1$, and $\alpha = 1$. Figure 11a shows the frequency response of the true dynamic model G, and the identified model using RCO. For nonparametric identification of $\mathcal{H}$, $m = 500$ and $A_0 = 0.919$. Figure 11b compares with true nonlinearity and the identified nonlinearity estimated using input reconstruction.

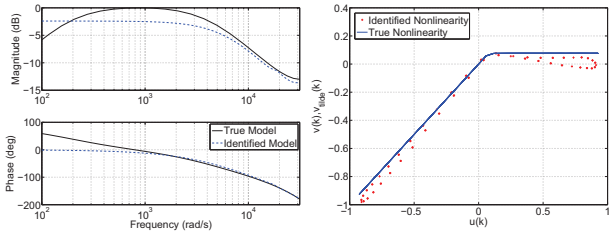

(a) (b)

Fig. 11. (a) Frequency response comparison of the true G and the identified LTI system the lines for the true and identified models almost coincide. (b) Identified nonlinearity versus true nonlinearity, where $m = 500$ and $A_0 = 0.919$. The argument of the identified nonlinearity is scaled by $\frac{1}{|G(e^{j\Omega_0})|}$ to facilitate comparison with the true nonlinearity (20)

Example 6.3: (Diode in Parallel with RLC Circuit) We now revisit the diode problem without using RCO, by fitting an output error model (OEM) of the form

$$y(k) = \frac{B(\mathbf{z})}{F(\mathbf{z})}u(k) + e(k), \tag{21}$$

where $B(\mathbf{z})$ and $F(\mathbf{z})$ are polynomials. The coefficients of $B(\mathbf{z})$, and $F(\mathbf{z})$ are determined by minimizing the error term $e(k)$, using a maximum likelihood method.

Figure 12a shows the frequency response of the true dynamic model G and the identified model using the OEM fit. The identified nonlinearity using input reconstruction and the actual nonlinearity are shown in Figure 12b.

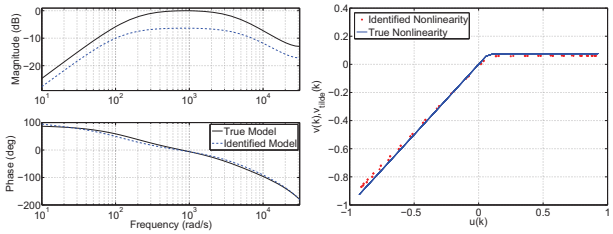

(a) (b)

Fig. 12. (a) Frequency response comparison of the true G and the identified LTI system, where the identified linear system is an output error model (OEM) fit (b) Identified nonlinearity versus true nonlinearity, where $m = 500$ and $A_0 = 5$. The argument of the identified nonlinearity is scaled by $\frac{1}{|G(e^{j\Omega_0})|}$ to facilitate comparison with the true nonlinearity (20)

VII. Conclusion

In this paper we develop a two-step method to identify semiparametric models for SISO discrete-time Hammerstein systems. We assume that the linear dynamic block is asymptotically stable, and the static nonlinearity is piecewise continuous.

First, we identify a parametric model of the linear dynamic system using a sufficiently rich input. We identify the parametric model using retrospective cost optimization and, in one example, using an output error model.

Second, we choose a single harmonic input and measure the system output when the state trajectory is in harmonic steady state. Using the system output and input reconstruction we estimate the intermediate signal, which may be shifted compared to the true intermediate signal, since the relative degree of the linear system is unknown. We exploit symmetry properties of the estimated intermediate signal compared to the input, which we use to approximate the nonharmonic phase shift and, therefore, estimate the delay between the estimate and true intermediate signal. Using the estimate of the intermediate signal, a nonparametric model of the static nonlinearity is obtained.

This method is effectively demonstrated on two simulated examples. Furthermore, two experimental examples are presented, namely, an RLC circuit with saturation at the input, and an RLC circuit containing a diode.

References

[1] L. A. Aguirre, M. C. S. Coelho, and M. V. Corrêa. On the Interpretation and Practice of Dynamical Differences between Hammerstein and Wiener Models. *IEE Proc. - Control Theory Appl.*, v. 152, n. 4, pp. 349–356, 2005.

[2] E. W. Bai and J. Reyland. Towards Identification of Wiener Systems with the Least Amount of *a Priori* Information: IIR cases. *Automatica*, v. 45, pp. 956–964 2009.

[3] E. W. Bai. Frequency Domain Identification of Wiener Models. *Automatica*, Vol. 39, n. 9, pp. 1521–1530, 2003.

[4] P. Crama and J. Schoukens. Initial Estimates of Wiener and Hammerstein Systems Using Multisine Excitation. *IEEE Trans. Instrum. Meas.*, Vol. 50, n. 6, pp. 1791–1795, 2001.

[5] A. M. D'Amato, B. O. S. Teixeira, and D. S. Bernstein. Semiparametric Identification of Wiener Systems Using a Single Harmonic Input and Retrospective Cost Optimization. *Proc. ACC 2010*, pp. 4812–4817 Baltimore, MD, June-July, 2010.

[6] W. Greblicki and M. Pawlak. *Nonparametric System Identification*, Cambridge University Press, 2008.

[7] J. B. Hoagg, M. A. Santillo, and D. S. Bernstein. Discrete-Time Adaptive Command Following and Disturbance Rejection for Minimum Phase Systems with Unknown Exogenous Dynamics. *IEEE Trans. Autom. Contr.*, Vol. 53, n. 4, pp. 912–928, 2008.

[8] M. A. Santillo and D. S. Bernstein, "Adaptive Control Based on Retrospective Cost Optimization," *AIAA J. Guid. Contr. Dyn.*, Vol. 33, pp. 289–304, 2010.

[9] M. A. Santillo, A. M. D'Amato, and D. S. Bernstein. System Identification Using a Retrospective Correction Filter for Adaptive Feedback Model Updating. *Proc. ACC 2009*, pp. 4392–4397, St. Louis, MO, June, 2009.

[10] J. Wang, Q. Zhang, and L. Ljung. Revisiting Hammerstein System Identification Through the Two-Stage Algorithm for Bilinear Parameter Estimation. *Automatica*, Vol. 45, n. 11, pp. 2627–2633, 2009.

[11] R. Venugopal and D. S. Bernstein. Adaptive Disturbance Rejection Using ARMARKOV System Representations. *IEEE Trans. Contr. Sys. Tech.*, Vol. 8, pp. 257–269, 2000.

[12] S. Kirtikar, H. Palanthandalam-Madapusi, E. Zattoni, and D. S. Bernstein, "l-Delay Input Reconstruction for Discrete-Time Systems," *Proc. Conf. Dec. Contr.*, pp. 1848–1853, Shanghai, China, December 2009.

[13] G. Marro, E. Zattoni, "Unknown-state, unknown-input reconstruction in discrete-time nonminimum-phase systems: Geometric methods," *Automatica*, Vol. 46, n.11, pp. 815-822, 2010.

[14] L. Ljung, *System Identification: Theory for the User*, 2nd edition, Prentice Hall, 1999.

[15] A. A. Ali, A. M. D'Amato, and D. S. Bernstein, "On the Accuracy of Least Squares Identification for Hammerstein Systems," *Proc. Amer. Contr. Conf.*, San Francisco, CA, June 2011. (submitted)